

## Facial synthesis of two-dimensional $\text{In}_2\text{S}_3/\text{Ti}_3\text{C}_2\text{T}_x$ heterostructures with boosted photoactivity for the hydrogenation of nitroaromatic compounds

Yisong Zhu<sup>a</sup>, Guanshun Xie<sup>a</sup>, Guohao Li<sup>a</sup>, Fei Song<sup>a</sup>, Changqiang Yu<sup>a</sup>, Zhenjun Wu<sup>b,\*</sup>, Xiuqiang Xie<sup>a,\*</sup>, Nan Zhang<sup>a,\*</sup>

<sup>a</sup> College of Materials Science and Engineering, Hunan Joint International Laboratory of Advanced Materials and Technology for Clean Energy, Hunan University, P. R. China.

<sup>b</sup> College of Chemistry and Chemical Engineering, Hunan University, P. R. China.

\*Corresponding authors.

*E-mail: xiuqiang\_xie@hnu.edu.cn; nanzhang@hnu.edu.cn; wooawt@163.com.*

### Contents list

**Fig. S1.** SEM images of bare  $\text{In}_2\text{S}_3$ .

**Fig. S2.** Contact angle of  $\text{Ti}_3\text{C}_2\text{T}_x$  nanosheets.

**Fig. S3.** SEM images of  $\text{In}_2\text{S}_3/\text{Ti}_3\text{C}_2\text{T}_x$ -1% at 95 °C for different refluxing time: (a) 0.5 h; (b) 4 h; (c) 5 h and different content  $\text{Ti}_3\text{C}_2\text{T}_x$ : (d) 5%, (e) 20%, (f) 30%.

**Fig. S4.** Raman spectra of bare  $\text{In}_2\text{S}_3$  and  $\text{In}_2\text{S}_3/\text{Ti}_3\text{C}_2\text{T}_x$ -1%.

**Fig. S5.** UV-vis DRS of as-obtained samples (the inset: photographs of each sample).

**Fig. S6.** XPS spectra of  $\text{Ti}_3\text{C}_2\text{T}_x$  and  $\text{In}_2\text{S}_3/\text{Ti}_3\text{C}_2\text{T}_x$ -1%.

**Fig. S7.** Transient photocurrent spectra of as as-obtained samples.

**Fig. S8.** The XPS spectra of  $\text{In}_2\text{S}_3/\text{Ti}_3\text{C}_2\text{T}_x$ -1% before and after photocatalysis.

**Fig. S9.** Nitrogen ( $\text{N}_2$ ) adsorption-desorption isotherms of bare  $\text{In}_2\text{S}_3$  and  $\text{In}_2\text{S}_3/\text{Ti}_3\text{C}_2\text{T}_x$ -1%.

**Fig. S10.** Decay curves of photovoltage of  $\text{In}_2\text{S}_3$  and  $\text{In}_2\text{S}_3/\text{Ti}_3\text{C}_2\text{T}_x$ -1%.

**Fig. S11.** The estimated band gap energy (a) of  $\text{In}_2\text{S}_3$  based on the Kubelka-Munk function plot transformed from the absorbance; VB-XPS spectra (b) and Mott-Schottky curves (c) of  $\text{In}_2\text{S}_3$ .

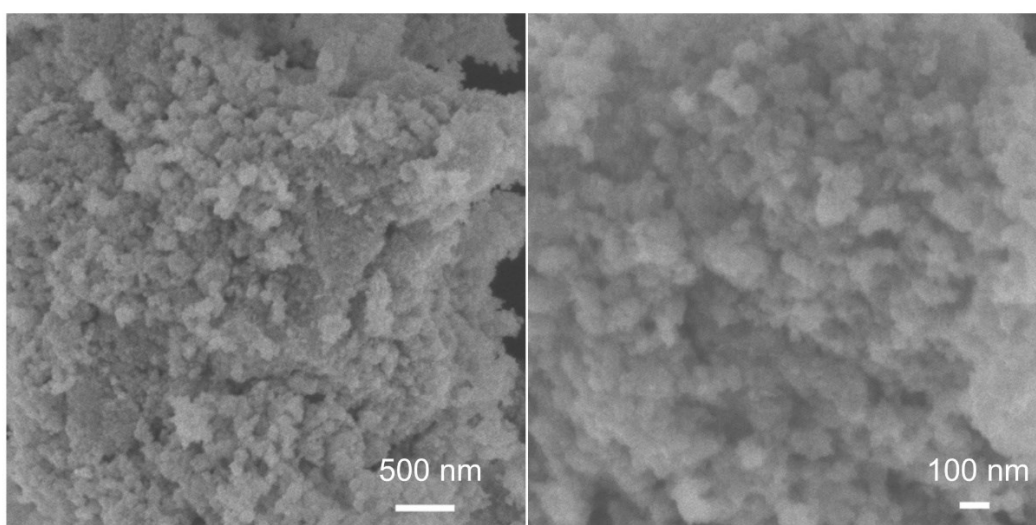


Fig.S1. SEM images of bare  $\text{In}_2\text{S}_3$ .



Fig.S2. Contact angle of  $\text{Ti}_3\text{C}_2\text{T}_x$  nanosheets.

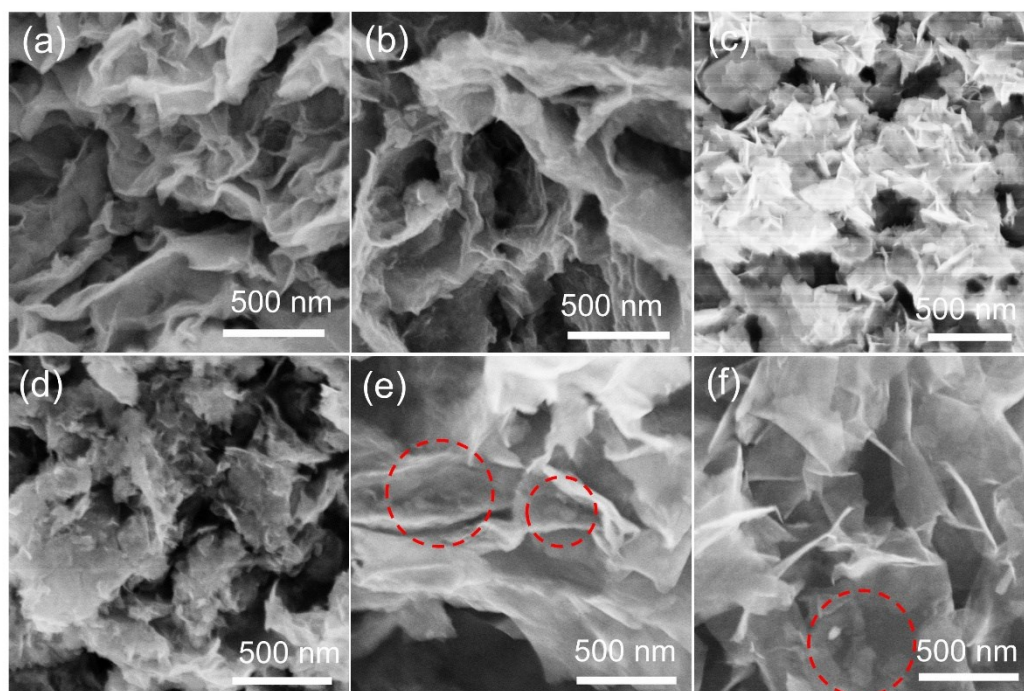


Fig.S3. SEM images of  $\text{In}_2\text{S}_3/\text{Ti}_3\text{C}_2\text{T}_x$ -1% at  $95\text{ }^\circ\text{C}$  for different refluxing time: (a) 0.5 h; (b) 4 h; (c) 5 h and different content  $\text{Ti}_3\text{C}_2\text{T}_x$ : (d) 5%, (e) 20%, (f) 30%.

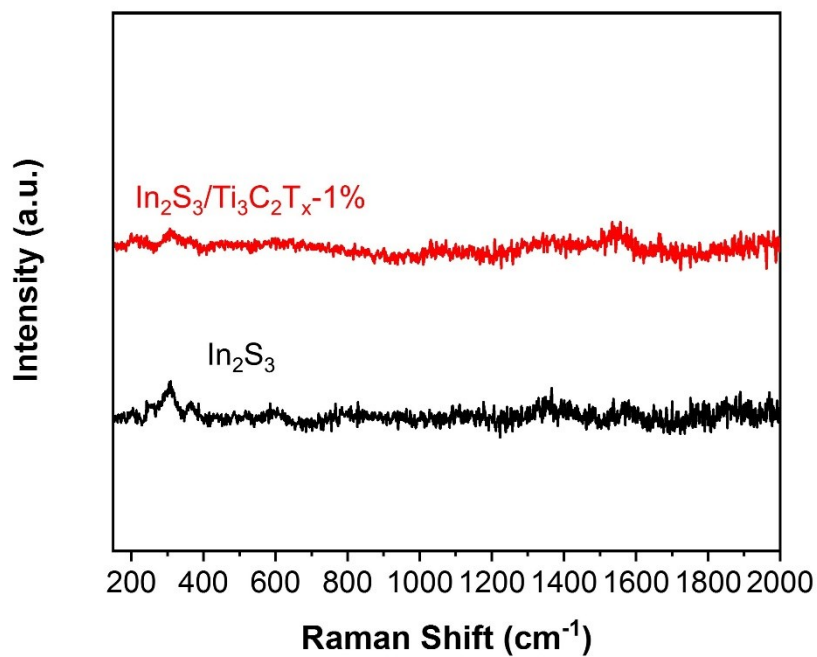


Fig. S4. Raman spectra of bare In<sub>2</sub>S<sub>3</sub> and In<sub>2</sub>S<sub>3</sub>/Ti<sub>3</sub>C<sub>2</sub>T<sub>x</sub>-1%.

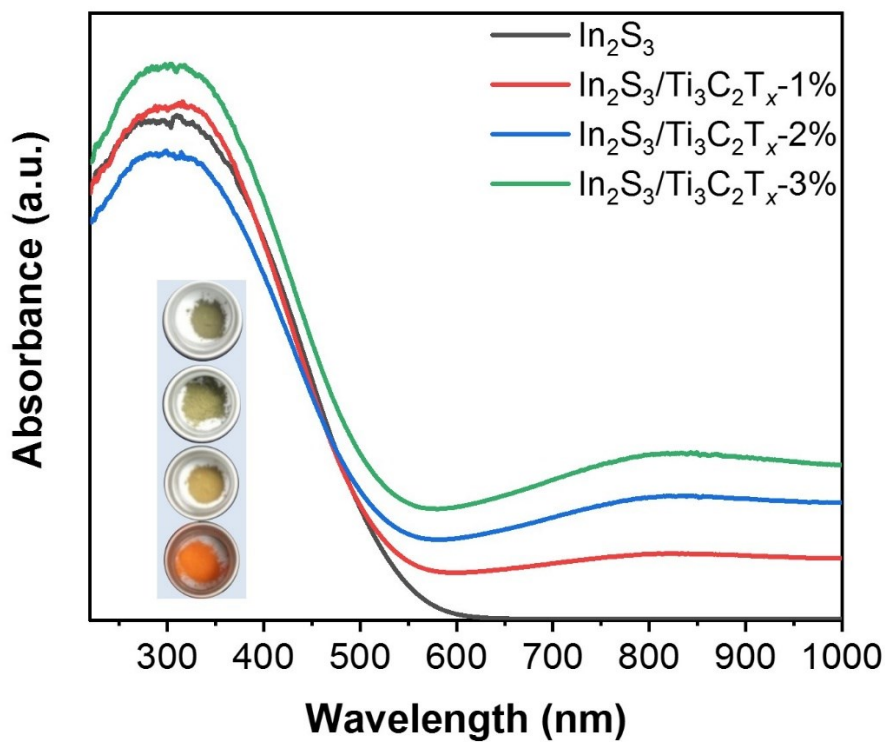


Fig. S5. UV-vis DRS of as-obtained samples (the inset: photographs of each sample).

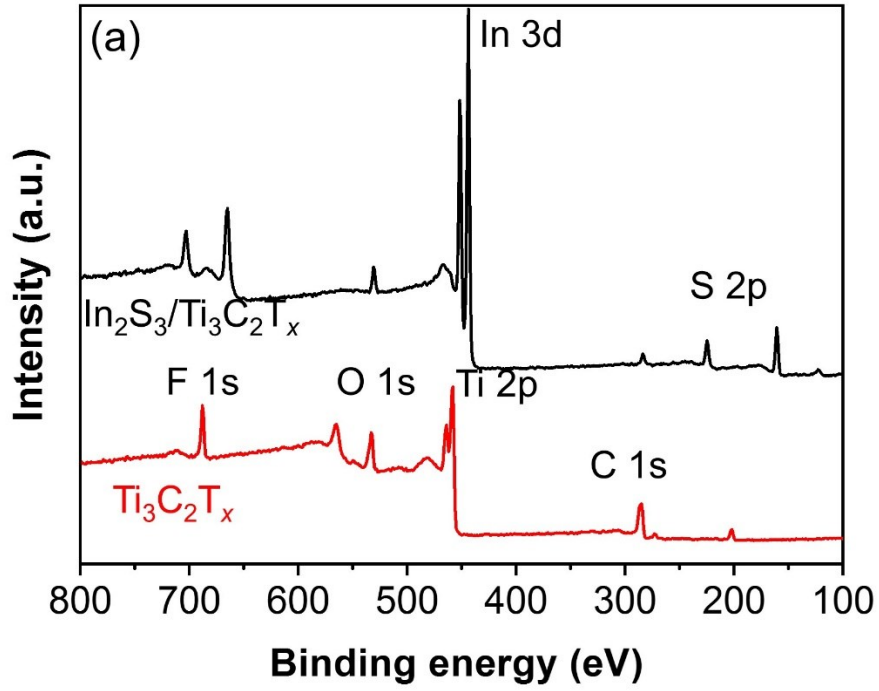


Fig. S6. XPS spectra of  $\text{Ti}_3\text{C}_2\text{T}_x$  and  $\text{In}_2\text{S}_3/\text{Ti}_3\text{C}_2\text{T}_x$ -1%.

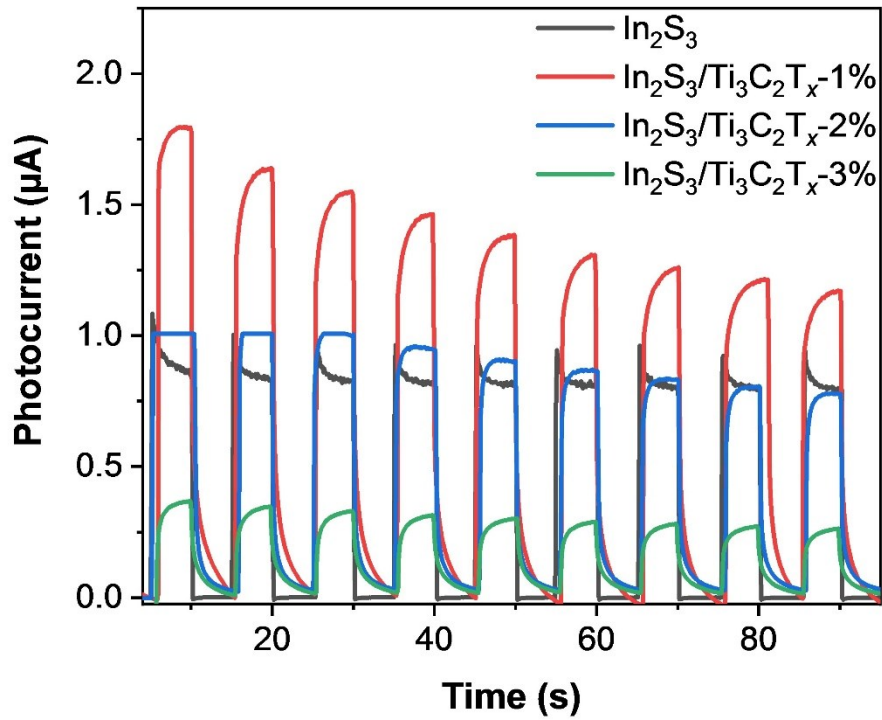


Fig.S7. Transient photocurrent spectra of as as-obtained samples.

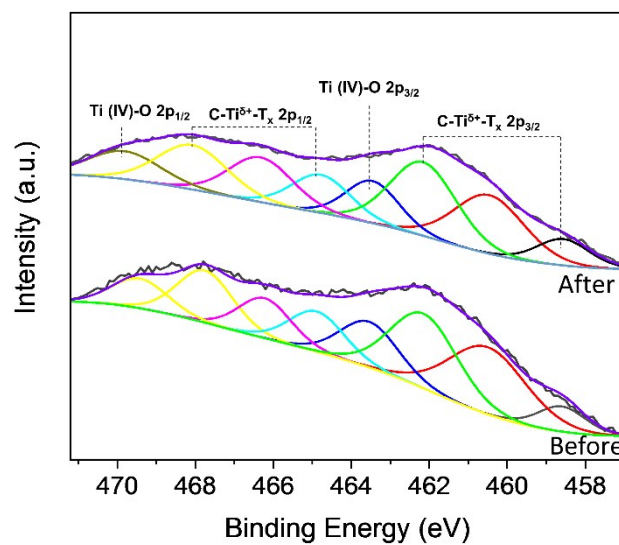


Fig. S8. The XPS spectra of  $\text{In}_2\text{S}_3/\text{Ti}_3\text{C}_2\text{T}_x-1\%$  before and after photocatalysis.

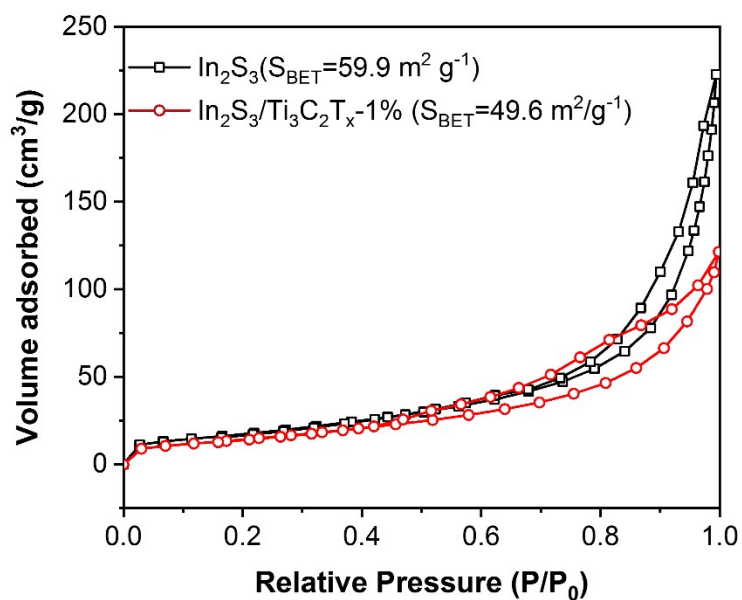


Fig. S9. Nitrogen ( $\text{N}_2$ ) adsorption-desorption isotherms of bare  $\text{In}_2\text{S}_3$  and  $\text{In}_2\text{S}_3/\text{Ti}_3\text{C}_2\text{T}_x-1\%$ .

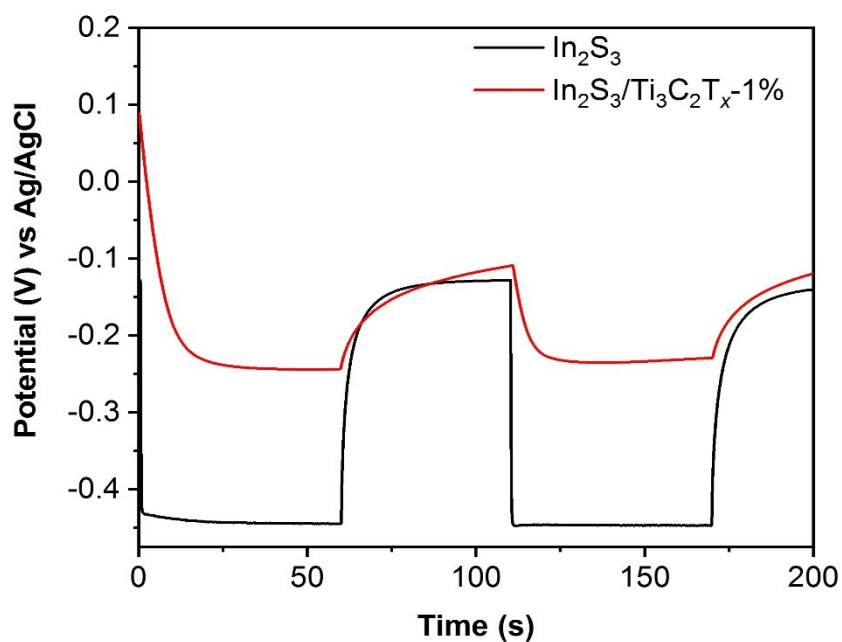


Fig. S10. Decay curves of photovoltage of  $\text{In}_2\text{S}_3$  and  $\text{In}_2\text{S}_3/\text{Ti}_3\text{C}_2\text{T}_x-1\%$ .

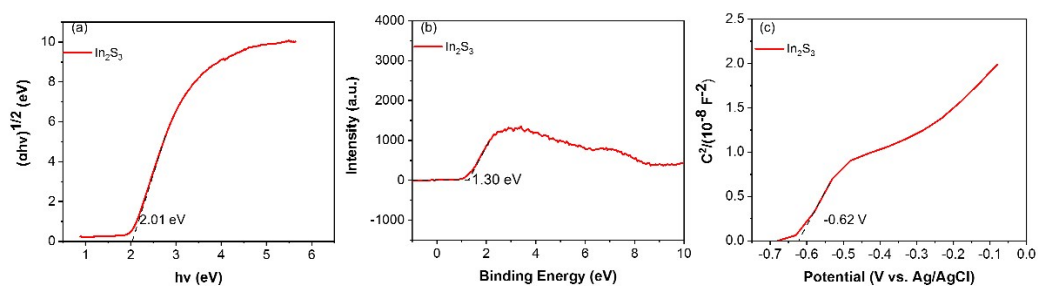


Fig. S11. The estimated band gap energy (a) of  $\text{In}_2\text{S}_3$  based on the Kubelka-Munk function plot transformed from the absorbance; VB-XPS spectra (b) and Mott-Schottky curves (c) of  $\text{In}_2\text{S}_3$ .